

Methods

1. Mann-Kendall test and Sen's slope estimator– trend detection

The non-parametric Mann-Kendall test is widely used in detecting trends of variables in meteorology and hydrology fields [1–3]. Statistic S can be obtained by Eq.(1).

$$S = \sum_{k=1}^{n-1} \sum_{j=k+1}^n \text{sgn}(x_j - x_k) \quad (1)$$

$$\text{sgn}(x_j - x_k) = \begin{cases} +1, & \text{if } (x_j - x_k) > 0 \\ 0, & \text{if } (x_j - x_k) = 0 \\ -1, & \text{if } (x_j - x_k) < 0 \end{cases} \quad (2)$$

where n is the length of the sample, x_k and x_j are from $k=1, 2, \dots, n-1$ and $j=k+1, \dots, n$. If n is bigger than 8, statistic S approximates to normal distribution. The mean of S is 0 and the variance of S can be acquired as follows:

$$\text{var}(S) = \frac{n(n-1)(2n+5)}{18} \quad (3)$$

Then the test statistic Z is denoted by Eq.(4).

$$Z = \begin{cases} \frac{S-1}{\sqrt{\text{var}(S)}}, & \text{if } S > 0 \\ 0, & \text{if } S = 0 \\ \frac{S+1}{\sqrt{\text{var}(S)}}, & \text{if } S < 0 \end{cases} \quad (4)$$

If $Z > 0$, it indicates an increasing trend, and vice versa. Given a confidence level α , the sequential data would be supposed to experience statistically significant trend if $|Z| > Z(1-\alpha/2)$, where $Z(1-\alpha/2)$ is the corresponding value of $P=\alpha/2$ following the standard normal distribution. In this study, 0.05 and 0.01 confidence levels were used.

Besides, the magnitude of a time series trend was evaluated by a simple non-parametric procedure developed by Sen [4]. The trend is calculated by

$$\beta = \text{Median}\left(\frac{x_j - x_i}{j - i}\right), \quad j > i \quad (5)$$

where β is Sen's slope estimate. $\beta > 0$ indicates upward trend in a time series. Otherwise the data series presents downward trend during the time period.

2. Mann-Kendall test - mutation detection

Mann-Kendall test can also be used to detect the abrupt changes of climate and hydrological data [5–8]. First, building an order serial S_k :

$$S_k = \sum_{i=1}^k \sum_{j=i+1}^n a_{ij} \quad (k = 2, 3, \dots, n) \quad (6)$$

where $a_{ij} = 1$ when $x_i > x_j$; $a_{ij} = 0$ when $x_i \leq x_j$.

Test statistic can be expressed as:

$$UF_k = [S_k - E(S_k)]/[Var(S_k)] \quad (k = 1, 2, \dots, n) \quad (7)$$

where $E(S_k) = n(n - 1/4)$; $Var(S_k) = n(n - 1)(2n + 5)/72$. UF_k is the forward sequence and follows the normal distribution. UB_k can then be denoted by reversing the series of data based on the same equation.

The null hypothesis (no abrupt change point) will be rejected if the UF_k values are greater than the confidence interval, and the approximate time of occurrence of the change point can be located according to the intersection between UF_k and UB_k within the confidence interval. If the intersection is outside the confidence interval, we need to employ another method (a moving t-test technique was used for this study) to analyze the stationarity of hydrometeorological data again.

3. Moving t-test technique

The moving t-test technique was adopted to detect change point by evaluating significant difference between two samples, and has been extensively used [2,9]. This method divides one random variable into two consecutive subsets x_1 and x_2 , where u_i , s_i^2 and n_i represent the mean value, variance and sample size of x_i ($i = 1, 2$), respectively. The procedures are as follows:

Null hypothesis: $H_0: u_1 - u_2 = 0$. Statistic t_0 is defined by Equation (8).

$$t_0 = \frac{\bar{x}_1 - \bar{x}_2}{s_p(1/n_1 + 1/n_2)^{1/2}} \quad (8)$$

where s_p is:

$$s_p = \sqrt{\frac{n_1 s_1^2 + n_2 s_2^2}{n_1 + n_2 - 2}} \quad (9)$$

t_0 complies with the t-distribution with degree of freedom $v = n_1 + n_2 - 2$. The null hypothesis would be rejected once $|t_0| \geq t_\alpha$ at a significant level α . It means that there is an abrupt change in the sample series. Because different choice of the subsets length can affect the location of turning point, a typical significant level of 0.05 and two conditions $n_1 = n_2 = 10$ and $n_1 = n_2 = 15$ were chosen in this study.

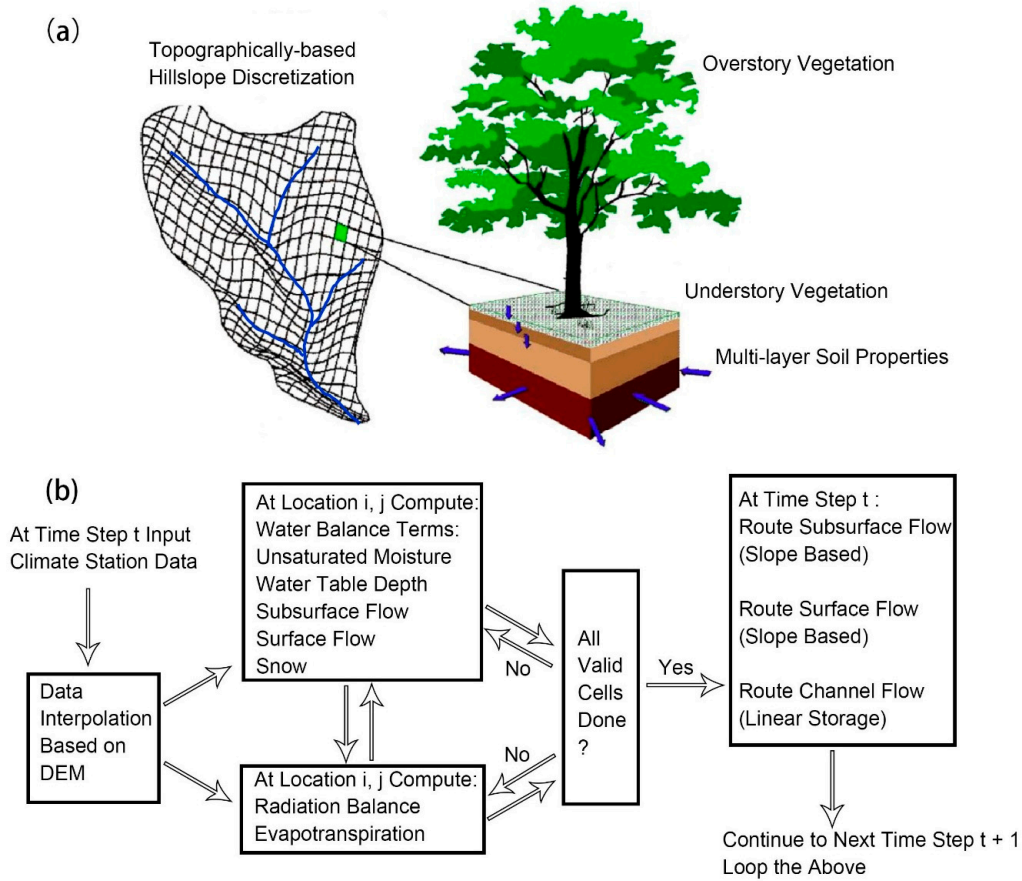


Figure S1. Conceptual representation (a) and flow chart (b) of DHSVM. (Flow chart is from [10]).

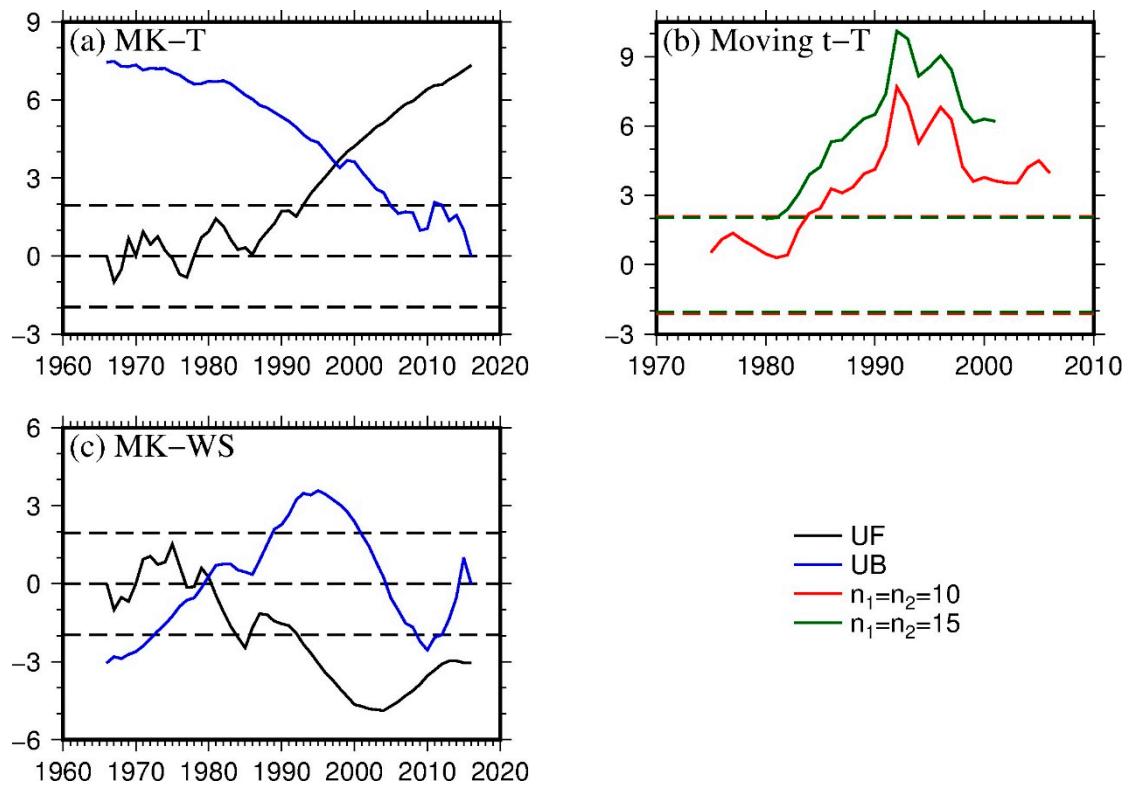


Figure S2. Change-point detection of annual data. Mann-Kendall test on annual temperature at DT (T, a), moving t-test technique applied to annual temperature at DT (T, b), Mann-Kendall test on annual wind speed at DT (WS, c).

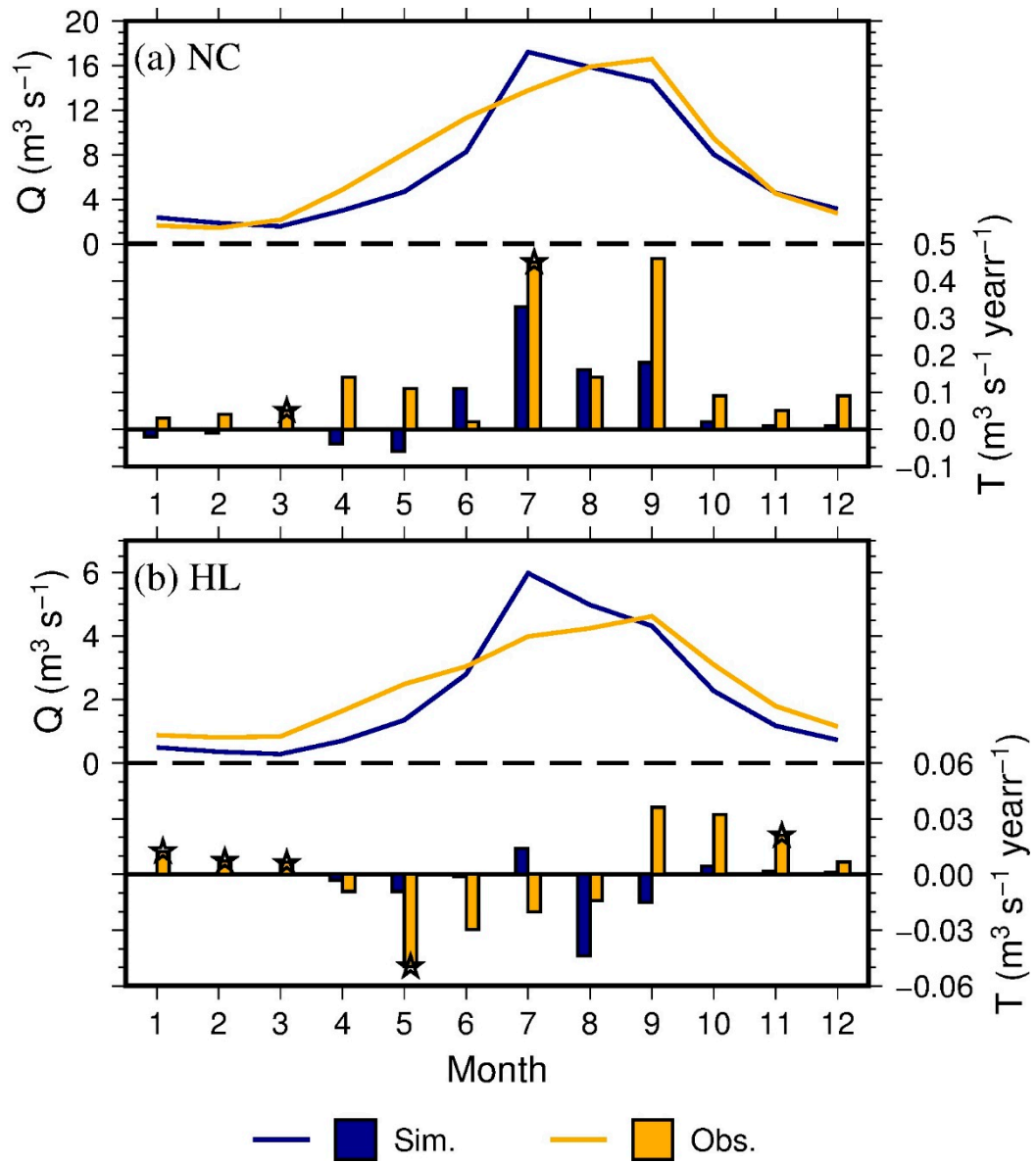


Figure S3. Means and trends of monthly streamflow for simulation and observation at NC (2002-2016) and HL (1981-2016).

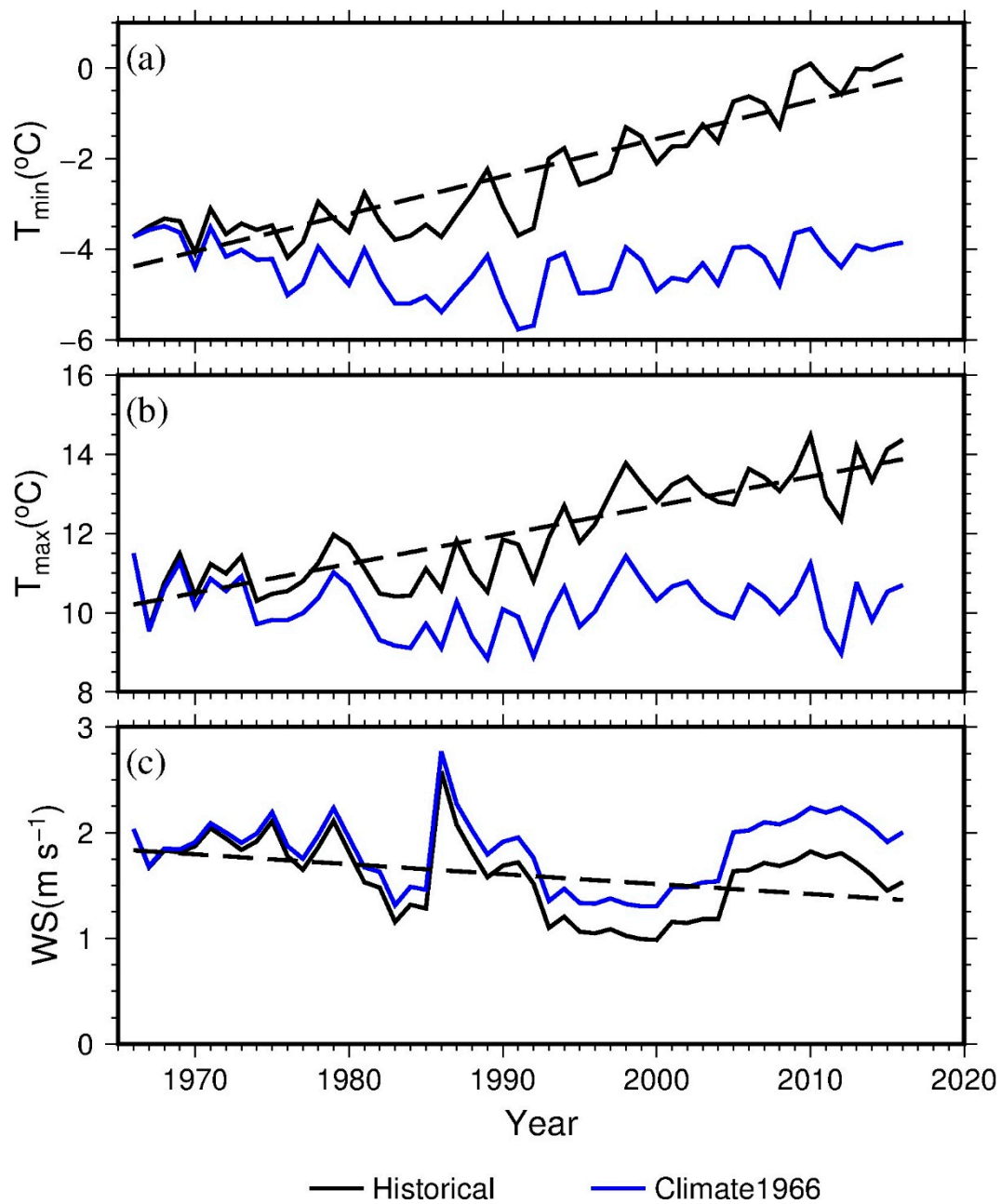


Figure S4. Minimum and maximum temperature, wind speed for historical period 1966-2016 and climate 1966 for Datong station.

Table S1. Transition matrix of land use in the Beichuan River Basin from 1980 to 2000 (km²).

Land Use Types		2000							Total
		Woodland	Wooded Grassland	Closed Shrubland	Grassland	Cropland	Bare Ground	Urban and Built	
1980	Woodland	102.04	0.69	1.25	8.95	3.86		0.19	117.04
	Wooded grassland	0.28	98.58	1.25	12.24	1.82	0.02	0.59	114.82
	Closed shrubland	0.85	1.32	542.94	69.01	5.61	0.40	0.07	620.59
	Grassland	5.52	7.81	42.62	1254.50	26.46	29.88	5.20	1372.04
	Cropland	5.06	2.66	5.76	38.03	289.51		15.44	358.52
	Bare ground			0.41	32.74		165.70		198.85
	Urban and built	0.12	0.05	0.04	2.09	4.29		19.86	26.44
	Water		0.06			1.60		0.29	3.29
	Total	113.87	111.17	594.26	1417.56	333.15	196.01	41.65	2811.59

Table S2. Transition matrix of land use in the Beichuan River Basin from 2000 to 2015 (km²).

Land Use Types		2015							Total
		Woodland	Wooded Grassland	Closed Shrubland	Grassland	Cropland	Bare Ground	Urban and Built	
2000	Woodland	113.57		0.02	0.03			0.03	113.87
	Wooded grassland		111.13			0.01		0.02	111.17
	Closed shrubland	0.79		591.10	1.50	0.20			594.26
	Grassland	1.04	0.13	0.01	1415.70	0.06	0.02	0.11	1417.55
	Cropland		0.01	0.14	0.10	326.83		3.17	333.15
	Bare ground				6.61		189.40		196.01
	Urban and built	0.01	0.04		0.02	0.10		41.48	41.65
	Water	0.01		0.04		0.02		0.02	3.92
	Total	115.42	111.31	591.30	1423.97	327.22	189.42	44.83	2811.59

References

- Ahn, K.H.; Merwade, V. Quantifying the relative impact of climate and human activities on streamflow. *J. Hydrol.* **2014**, *515*, 257-266.
- Liang, L.; Li, L.; Liu, Q. Temporal variation of reference evapotranspiration during 1961–2005 in the Taoer River basin of Northeast China. *Agr. Forest Meteorol.* **2010**, *150*, 298-306.
- Wang, X.; He, K.; Dong, Z. Effects of climate change and human activities on runoff in the Beichuan River Basin in the northeastern Tibetan Plateau, China. *Catena* **2019**, *176*, 81-93.
- Sen, P.K.J.J.o.t.A.s.a. Estimates of the regression coefficient based on Kendall's tau. *J. Am. Stat. Assoc.* **1968**, *63*, 1379-1389.
- Li, L.-J.; Zhang, L.; Wang, H.; Wang, J.; Yang, J.-W.; Jiang, D.-J.; Li, J.-Y.; Qin, D.-Y. Assessing the impact of climate variability and human activities on streamflow from the Wuding River basin in China. *Hydrol. Process.* **2007**, *21*, 3485-3491.
- Tian, F.; Yang, Y.H.; Han, S.M. Using runoff slope-break to determine dominate factors of runoff decline in Hutuo River Basin, North China. *Water Sci. Technol.* **2009**, *60*, 2135-2144.
- Ye, X.; Zhang, Q.; Liu, J.; Li, X.; Xu, C.Y. Distinguishing the relative impacts of climate change and human activities on variation of streamflow in the Poyang Lake catchment, China. *J. Hydrol.* **2013**, *494*, 83-95.
- Zhang, X.; Li, P.; Li, D. Spatiotemporal Variations of Precipitation in the Southern Part of the Heihe River Basin (China), 1984–2014. *Water* **2018**, *10*, 410.
- Zhao, Y.; Zou, X.; Cao, L.; Yao, Y.; Fu, G. Spatiotemporal variations of potential evapotranspiration and aridity index in relation to influencing factors over Southwest China during 1960–2013. *Theor. Appl. Climatol.* **2017**, *133*, 711-726.
- Cuo, L.; Giambelluca, T.W.; Ziegler, A.D. Lumped parameter sensitivity analysis of a distributed hydrological model within tropical and temperate catchments. *Hydrol. Process.* **2011**, *25*, 2405-2421.